Electronic Supplementary Information

1. Full author list of Ref. 88

M. J. Frisch, G. W. Trucks, H. B. Schlegel, G. E. Scuseria, M. A. Robb, J. R. Cheeseman, J. A. Montgomery, Jr., T. Vreven, K. N. Kudin, J. C. Burant, J. M. Millam, S. S. Iyengar, J. Tomasi, V. Barone, B. Mennucci, M. Cossi, G. Scalmani, N. Rega, G. A. Petersson, H. Nakatsuji, M. Hada, M. Ehara, K. Toyota, R. Fukuda, J. Hasegawa, M. Ishida, T. Nakajima, Y. Honda, O. Kitao, H. Nakai, M. Klene, X. Li, J. E. Knox, H. P. Hratchian, J. B. Cross, V. Bakken, C. Adamo, J. Jaramillo, R. Gomperts, R. E. Stratmann, O. Yazyev, A. J. Austin, R. Cammi, C. Pomelli, J. W. Ochterski, P. Y. Ayala, K. Morokuma, G. A. Voth, P. Salvador, J. J. Dannenberg, V. G. Zakrzewski, S. Dapprich, A. D. Daniels, M. C. Strain, O. Farkas, D. K. Malick, A. D. Rabuck, K. Raghavachari, J. B. Foresman, J. V. Ortiz, Q. Cui, A. G. Baboul, S. Clifford, J. Cioslowski, B. B. Stefanov, G. Liu, A. Liashenko, P. Piskorz, I. Komaromi, R. L. Martin, D. J. Fox, T. Keith, M. A. Al-Laham, C. Y. Peng, A. Nanayakkara, M. Challacombe, P. M. W. Gill, B. Johnson, W. Chen, M. W. Wong, C. Gonzalez, and J. A. Pople, *Gaussian 03*, Revision C.02, Gaussian, Inc., Wallingford CT, 2004.

2. Evolution with temperature of the absorption and emission spectra calculated for COOH-PTV

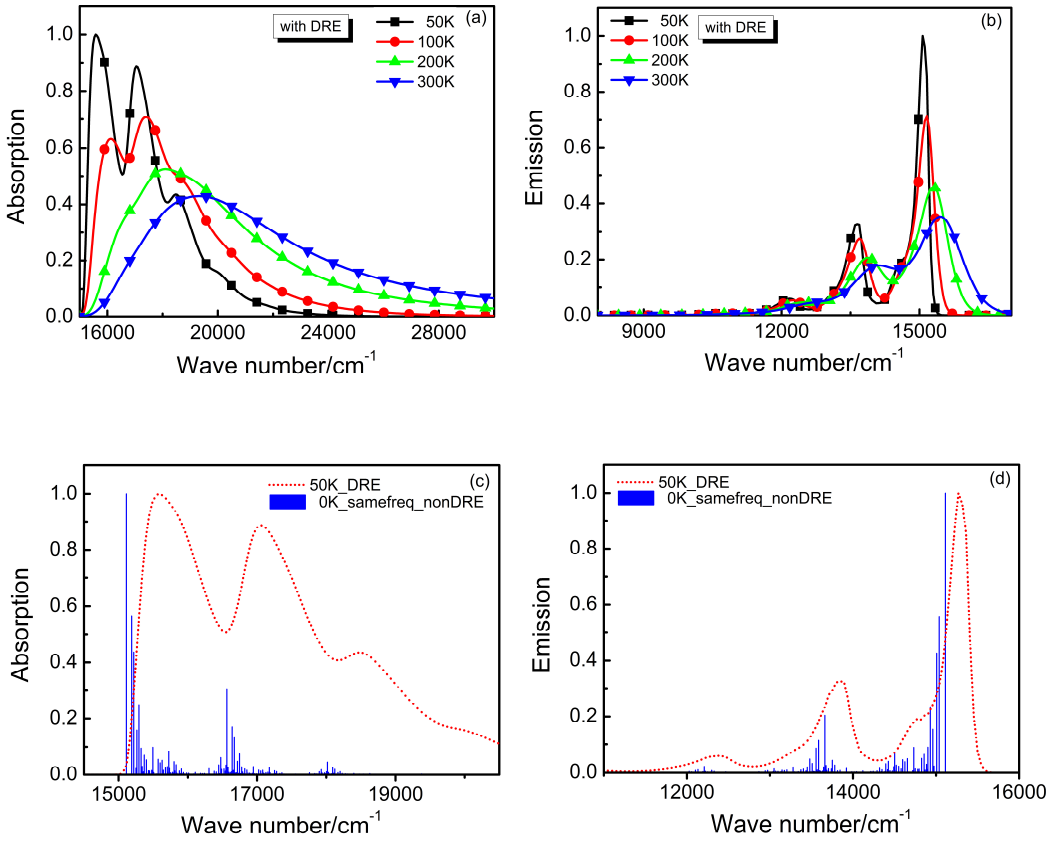

Fig. S1 The theoretical absorption (a) and emission (b) spectra with DRE and distortion effect at different temperatures and the theoretical absorption (c) and emission (d) spectra at 0K without DRE and distortion effect compared to the spectra at 50K with DRE and distortion effect.

We calculate a series of spectra at different temperatures for COOH-PTV (Fig. S1(a) and Fig. S1(b)) considering DRE with distortion effect. As temperature decreases, the mirror symmetry of absorption and emission gradually recovers. According to Boltzmann distribution, as temperature increases, the contribution from higher frequency modes of the initial state will increase.

Considering the normal mode frequencies in ground state and excited state are different, the evolution of the absorption and the emission spectra with temperature also becomes diffefrent. Figure S1(c) and Figure S1(d) present the spectra with the displaced but undisorted oscillator model at 0 K for COOH-PTV compared to the spectra with DRE with distortion effect at 50K. It is seen that the former satisfies the mirror symmetry. Thus, the observed spectra asymmetry is attributed to the potential energy surface distortion effect.

3. Ground state and excited state vibrational mode frequencies with Huang-Rhys factors for COOH-, NO_2-, and CHO-6TV.

Table S1. The frequencies and Huang-Rhys factors (HR) of ground state and excited state vibrational modes for COOH-6TV. Out of the total 240 normal modes, only the modes with HR larger than 1×10^{-4} are listed.

Mode order	S_0 Freq. (cm^{-1})	S_0 HR	S_1 Freq. (cm^{-1})	S_1 HR
1	16.67	0.0445	18.59	0.0535
2	38.54	0.0705	39.42	0.0836
3	75.62	0.5633	75.21	0.6190
4	105.63	0.4332	108.19	0.4042
5	121.02	0.0173	121.65	0.0262
6	138.45	0.0222	138.83	0.0204
7	198.54	0.0088	199.45	0.0088
8	226.63	0.0101	227.94	0.0107
9	245.58	0.0026	245.78	0.0026
10	262.15	0.0002	262.12	0.0001
11	307.66	0.0004	310.86	0.0002
12	372.48	0.0038	372.05	0.0031
13	376.10	0.0047	375.80	0.0076
14	381.59	0.0960	380.27	0.0965
15	421.20	0.0002	418.69	0.0001
16	423.66	0.0005	422.39	0.0002
17	507.56	0.0036	507.27	0.0031
18	515.84	0.0502	516.42	0.0461

19	606.30	0.0013	601.74	0.0072
20	611.96	0.0805	606.34	0.0698
21	677.96	0.0001	677.40	0.0001
22	694.66	0.0008	692.06	0.0008
23	736.72	0.0002	733.15	0.0002
24	758.98	0.0004	757.39	0.0003
25	828.96	0.0005	820.50	0.0010
26	880.29	0.0002	879.63	0.0002
27	898.43	0.0015	893.78	0.0010
28	924.16	0.0002	915.83	0.0007
29	940.73	0.0035	930.53	0.0034
30	1095.52	0.0022	1098.53	0.0006
31	1099.56	0.0030	1104.33	0.0000
32	1111.82	0.0002	1114.06	0.0002
33	1165.93	0.0045	1163.66	0.0025
34	1189.30	0.0001	1189.00	0.0004
35	1192.12	0.0005	1192.34	0.0020
36	1193.16	0.0204	1199.18	0.0132
37	1211.65	0.0001	1213.34	0.0002
38	1241.01	0.0011	1250.14	0.0019
39	1241.34	0.0022	1256.45	0.0056
40	1332.90	0.0331	1302.12	0.0221
41	1348.98	0.0004	1328.88	0.0142
42	1349.88	0.0023	1343.52	0.0004
43	1353.49	0.0000	1354.40	0.0048
44	1358.31	0.0002	1371.46	0.0160
45	1361.18	0.0570	1365.39	0.0393
46	1375.12	0.0177	1378.67	0.0010
47	1382.38	0.0089	1385.15	0.0002
48	1424.48	0.0004	1438.33	0.0001
49	1428.32	0.0114	1434.81	0.0031
50	1440.28	0.0027	1441.87	0.0013
51	1451.24	0.2762	1448.19	0.1255
52	1478.99	0.0089	1477.93	0.1116
53	1502.31	0.0000	1497.35	0.0017
54	1557.24	0.0035	1522.70	0.0297
55	1571.34	0.0098	1550.57	0.0116
56	1583.41	0.0018	1574.73	0.0005
57	1642.18	0.1088	1625.09	0.1084
58	1653.34	0.0003	1613.41	0.1074
59	1664.83	0.0116	1605.82	0.0001
60	1813.69	0.0003	1808.98	0.0001
61	1814.86	0.0001	1814.21	0.0001

Table S2. The frequencies and Huang-Rhys factors (HR) of ground state and excited state vibrational modes for NO_2-6TV. Out of total 222 normal modes, only the modes with HR larger than 1×10^{-4} are listed.

Mode order	S_0 Freq. (cm^{-1})	S_0 HR	S_1 Freq. (cm^{-1})	S_1 HR
1	17.30	0.0552	18.09	0.0619
2	38.84	0.0758	38.86	0.0916
3	78.40	0.5048	77.87	0.5590
4	108.00	0.4896	110.21	0.4519
5	132.31	0.0054	132.61	0.0088
6	149.66	0.0115	149.63	0.0101
7	205.44	0.0018	206.44	0.0020
8	237.61	0.0071	237.12	0.0081
9	257.31	0.0031	256.67	0.0030
10	265.17	0.0001	265.10	0.0000
11	383.64	0.0000	383.99	0.0018
12	388.86	0.0190	388.35	0.0190
13	396.69	0.0831	395.37	0.0827
14	425.30	0.0003	422.15	0.0024
15	432.65	0.0019	432.46	0.0032
16	529.99	0.0505	529.09	0.0190
17	531.25	0.0351	530.66	0.0611
18	551.76	0.0022	550.05	0.0027
19	589.58	0.0036	584.97	0.0039
20	614.81	0.0012	609.97	0.0070
21	621.98	0.0650	616.80	0.0540
22	733.83	0.0008	729.11	0.0009
23	754.84	0.0018	751.15	0.0012
24	782.93	0.0000	774.30	0.0001
25	795.20	0.0003	789.77	0.0001
26	808.88	0.0002	808.60	0.0001
27	873.57	0.0020	868.85	0.0031
28	884.53	0.0010	881.98	0.0004
29	900.61	0.0006	896.24	0.0003
30	945.10	0.0004	932.99	0.0012
31	954.28	0.0028	943.28	0.0016
32	1093.71	0.0087	1097.99	0.0031
33	1099.13	0.0000	1104.76	0.0003
34	1114.13	0.0013	1117.45	0.0011
35	1133.04	0.0001	1138.82	0.0001
36	1159.65	0.0001	1157.47	0.0002
37	1170.98	0.0037	1170.22	0.0027

38	1192.79	0.0006	1194.37	0.0007
39	1217.44	0.0001	1228.18	0.0016
40	1221.44	0.0089	1237.10	0.0101
41	1334.05	0.0129	1323.79	0.0102
42	1334.75	0.0148	1303.35	0.0212
43	1339.63	0.0022	1333.75	0.0020
44	1380.86	0.0029	1389.14	0.0004
45	1381.15	0.0026	1379.56	0.0039
46	1394.42	0.0196	1366.18	0.0021
47	1399.37	0.0268	1392.07	0.0004
48	1406.71	0.0710	1409.89	0.0677
49	1412.81	0.0018	1425.77	0.0249
50	1415.38	0.0001	1418.57	0.0586
51	1433.04	0.0015	1433.69	0.0012
52	1467.51	0.2301	1489.86	0.0887
53	1489.38	0.0170	1468.85	0.0239
54	1511.40	0.0000	1506.76	0.0015
55	1556.64	0.0057	1521.98	0.0652
56	1570.01	0.0079	1548.70	0.0108
57	1574.30	0.0042	1563.18	0.0002
58	1639.30	0.0851	1609.27	0.1053
59	1648.72	0.0000	1621.50	0.0640
60	1662.10	0.0240	1655.37	0.0058
61	1665.11	0.0001	1662.79	0.0020
62	1666.74	0.0062	1604.98	0.0099

Table S3. The frequencies and Huang-Rhys factors (HR) of ground state and excited state vibrational modes for CHO-6TV. Out of the total 222 normal modes, only those with HR larger than 1×10^{-4} are listed.

Mode order	S_0 Freq. (cm^{-1})	S_0 HR	S_1 Freq. (cm^{-1})	S_1 HR
1	18.48	0.0097	21.06	0.0115
2	46.31	0.0183	46.93	0.0268
3	74.62	0.5411	73.38	0.6074
4	119.06	0.5311	120.87	0.4825
5	143.16	0.0540	142.67	0.0648
6	172.19	0.0075	172.21	0.0076
7	201.94	0.0035	202.66	0.0040
8	229.94	0.0006	231.16	0.0006

9	252.90	0.0090	252.74	0.0075
10	263.85	0.0032	262.79	0.0032
11	310.79	0.0011	313.05	0.0010
12	409.31	0.0001	408.62	0.0000
13	424.98	0.0152	424.12	0.0154
14	462.59	0.0064	460.38	0.0075
15	475.45	0.0006	473.66	0.0000
16	476.73	0.0005	476.58	0.0017
17	576.26	0.0156	572.01	0.0196
18	595.95	0.0330	591.32	0.0151
19	609.28	0.1122	602.28	0.1204
20	689.52	0.0002	683.83	0.0001
21	696.26	0.0025	686.39	0.0019
22	705.57	0.0006	703.27	0.0004
23	740.83	0.0017	735.92	0.0016
24	767.71	0.0009	766.75	0.0005
25	841.34	0.0048	834.73	0.0065
26	864.45	0.0019	859.69	0.0019
27	895.78	0.0012	890.16	0.0022
28	896.40	0.0004	896.11	0.0001
29	976.82	0.0002	964.46	0.0002
30	985.65	0.0002	973.12	0.0000
31	999.59	0.0004	997.96	0.0004
32	1106.13	0.0035	1116.17	0.0005
33	1119.11	0.0035	1121.77	0.0023
34	1135.57	0.0039	1140.56	0.0012
35	1192.32	0.0200	1195.04	0.0094
36	1195.74	0.0039	1203.81	0.0104
37	1204.15	0.0002	1206.91	0.0002
38	1248.45	0.0002	1260.10	0.0000
39	1253.46	0.0002	1267.52	0.0010
40	1332.53	0.0269	1304.14	0.0193
41	1358.13	0.0385	1334.47	0.0376
42	1359.48	0.0045	1346.79	0.0065
43	1368.19	0.0003	1376.60	0.0008
44	1374.53	0.0007	1382.99	0.0002
45	1389.84	0.0006	1391.35	0.0003
46	1404.91	0.0033	1416.39	0.0044
47	1406.08	0.0030	1411.22	0.0050
48	1435.07	0.2439	1428.12	0.1226
49	1456.00	0.0012	1449.26	0.0586
50	1467.05	0.0084	1465.78	0.0002
51	1473.43	0.0326	1480.83	0.0353
52	1491.70	0.0002	1487.25	0.0000

53	1546.27	0.0098	1523.17	0.0455
54	1562.46	0.0124	1547.32	0.0163
55	1571.65	0.0017	1563.22	0.0004
56	1639.80	0.0973	1621.97	0.0822
57	1650.66	0.0005	1610.98	0.0968
58	1663.92	0.0112	1606.55	0.0061
59	1792.51	0.0002	1781.87	0.0000
60	1794.02	0.0001	1791.36	0.0000

The difference in frequencies and Huang-Rhys factors between ground state and excited state modes are the main reason which causes the mirror asymmetry in COOH-PTV's spectra.

4. Comparison of the optical spectra and the radiative/nonradiative decay rates for CHO-PTV to justify the approach to remove one mode with imaginary frequency

In Fig. S2, we depict the calculated optical absorption and emission spectra: F1 and F2 indicate without and with replacement of the out-of-plane mode in excited state by that of the ground state. They are basically identical. Such operation only causes slight change for the non-radiative decay rate, see Table S4.

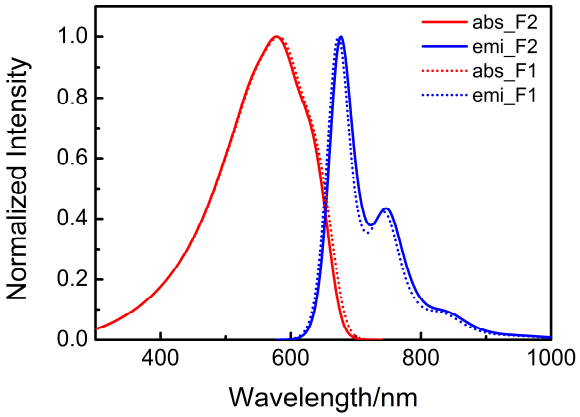

Fig. S2. The theoretical absorption and emission spectra of CHO-PTV resulted from F1 and F2.

Table S4. The theoretical radiative and nonradiative decay rates of CHO-PTV resulted from F1 and F2.

frequencies	F1	F2
k_r/s^{-1}	4.61×10^{8}	4.50×10^{8}
k_{IC}/s^{-1}	2.08×10^{6}	2.51×10^{6}